Influence of Jahn-Teller Cu^{2+} doping on the structural and magnetic properties of quasi-two-dimensional oxyborate $(Ni,Cu)_2MnBO_5$

Andrey Kartashev [a], Evgeniy Eremin [a,b], Evgeniya Moshkina [a], Maksim Molokeev [a], Svetlana Sofronova [a,*]

[a] *Kirensky Institute of Physics, Krasnoyarsk Scientific Center, Siberian Branch, Russian Academy of Sciences, Krasnoyarsk 660036, Russia*
[b] *Reshetnev Siberian State University of Science and Technology, 660037 Krasnoyarsk, Russia*

ABSTRACT

Using the flux technique single crystals of $(Ni,Cu)_2MnBO_5$ were grown. The crystal structure of this compound belongs to the space group Pbam(55). There are no monoclinic distortions of the crystal structure. The analysis of the structural data shows that the content of copper ions in the crystal is lower than 10 percent. The magnetic ordering into the ferrimagnetic phase occurs at 75 K. The assessment of the exchange interactions shows that changes in the exchange interactions lead to increasing frustrations in the system which could result in a decrease in the temperature of magnetic ordering.

1. Introduction

Crystals with the ludwigite structure have attracted the attention of scientists for a few last decades due to interesting physical properties appropriate to these crystals [1–4]. For example, the charge ordering is observed in Fe_3BO_5 [5]. The exchange bias of the hysteresis loops in a small temperature range is found in $Ni_5GeB_2O_{10}$ [6]. In $Mn_{3-x}Ni_xBO_5$ the reversal magnetization is observed for some values of x [7]. The crystal structure of these compounds has quasi-low dimensional elements which are zigzag walls. Here, metal ions form triangular groups, which generate a geometric prerequisite for frustrations appearing in the system. In Co_3BO_5, the magnetic ordering occurs at 42 K, but the Co^{3+} ions are in the low-spin state, their spins being almost zero [8]. In [9] it is suggested that the frustrations lead to the transition of Co^{3+} to the low-spin state.

In many ludwigites the magnetic system is split into two subsystems. In Fe_3BO_5 [5] the magnetic ordering of the subsystems occurs at 112 K and 74 K, whose magnetic moments are oriented orthogonally. In contrast to Fe_3BO_5, in Cu_2MnBO_5 there is a single magnetic phase transition which occurs at $T = 92$ K. The magnetic moments of two subsystems are oriented at an angle of 60 degrees [10,11].

It is known that there are $(Ni,Mn)_3BO_5$ compounds, where the manganese ions in different valence states are included in the crystals. $Ni_{2.5}Mn_{0.5}BO_5$ crystals were grown by Bluhm [12], $Ni_{2.14}Mn_{0.86}BO_5$ and

Ni_2MnBO_5 were grown by Bezmaternykh and Moshkina [13,14]. In the first compound the Mn ions must be in the tetravalent state, but only the structural investigation of this compound was carried out. In $Ni_{2.14}Mn_{0.86}BO_5$ the Mn ions are in the trivalent and tetravalent states, while in Ni_2MnBO_5 these are only in the trivalent state. The valence state of the Mn ions in these compounds was investigated using the X-ray diffraction and EXAFS techniques [13,14]. It is interesting to note that an increase in the chemical disorder in $Ni_{2.14}Mn_{0.86}BO_5$ as compared with Ni_2MnBO_5 results in an increase in the temperature of the magnetic ordering.

In this study we investigate the crystal growth, structural and magnetic characteristics of ludwigite $(Ni,Cu)_2MnBO_5$. We also consider the effect of the presence of bivalent copper ions on its physical properties.

2. Crystal growth

$(Ni,Cu)_2MnBO_5$ single crystals were grown by the flux technique. The flux system can be written as $Bi_2Mo_3O_{12}$:2.57 B_2O_3:2 Li_2O:0.33 Mn_2O_3:0.33 Ni_2O_3:0.66 CuO. The crystallization conditions and crystal growth process are similar to [13,14]. The grown single crystals were in the form of black needles with the size of about 4 mm in length and 0.1 mm in thickness (Fig. 1). The weight of one needle was ~0,5 mg.
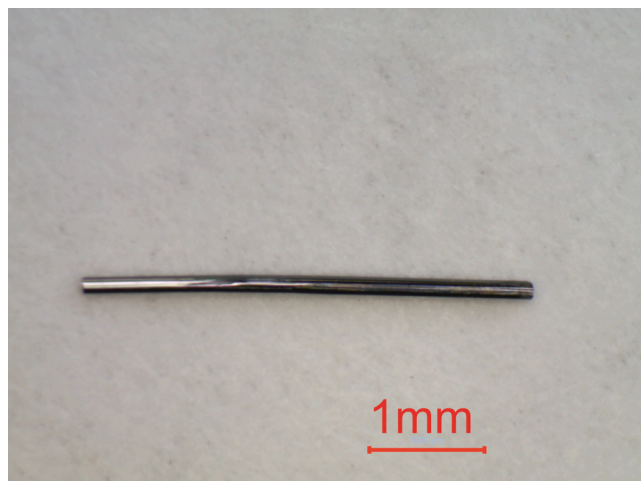

Fig. 1. The grown single crystal.

3. Structure

The crystal structure of the (Ni,Cu)2MnBO5 single crystal was investigated by the X-ray diffraction method at room temperature using a SMART APEXII diffractometer (Mo Kα, λ = 0.7106 Å). The crystal structure of $(Ni,Cu)_2MnBO_5$ belongs to the space group Pbam (D^9_{2h}) and has the ludwigite structure (Fig. 2). Its structure was refined by the least-square minimization using SHELX97 [15]. The unit cell contains 12 magnetic atoms occupying 4 nonequivalent positions: 2a, 2d, 4 h and 4 g (1–4 in Fig. 2, respectively) and involves four formula units. It is extremely difficult to specify the concentrations of Cu, Ni and Mn ions in different positions using the X-ray diffraction method. Therefore, the designation "Me" is used which means Cu/Mn/Ni.

In order to estimate the distribution of metallic ions over the positions we have to analyze the cell parameters and other structural parameters, which are given in Tables 1 and 2. The comparison of the structural data of the parent compounds (Ni_2MnBO_5 and Cu_2MnBO_5) and studied samples (Table 2) allows us to make an assumption on the distribution of the metallic ions over the positions. We suggest that the Mn ions are only trivalent and they occupy the Me_4 position due to the Ni and Cu ions being both bivalent. The positions Me_1-Me_3 are occupied by the Ni and Cu ions.

With the space group of the parent compounds being different, the correspondence of the positions in different space groups (*Pbam* and $P2_1/c$) is given in [10]. The crystal cell of the studied samples is orthorhombic. This indicates that the concentration of Cu ions in the
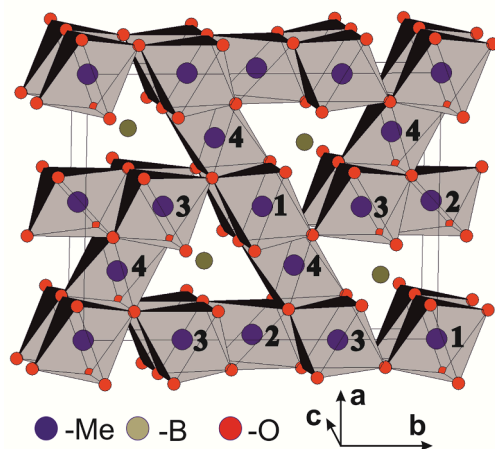
Table 1
The coordinates of the ions of the studied sample.

Atom	Wyckoff index	x/a	y/b	z/c
Me1	2a	0	0	0
Me2	2d	1/2	0	1/2
Me3	4 g	0.99851(4)	0.28029(4)	0
Me4	4 h	0.76055(5)	0.11582(4)	1/2
B	4 h	0.7235(4)	0.3621(3)	1/2
O1	4 g	0.8939(3)	0.1436(2)	0
O2	4 h	0.6476(3)	0.2642(2)	1/2
O3	4 h	0.8517(3)	0.0415(2)	1/2
O4	4 g	0.6129(3)	0.0805(2)	0
O5	4 h	0.8738(3)	0.3596(2)	1/2

Table 2
The cell and geometric parameters.

	Pbam	P2₁/c	(Ni,Cu)₂MnBO₅ Pbam	Ni₂MnBO₅ Pbam	Cu₂MnBO₅ P2₁/c
Bonds	Number of bonds		d(Å)		
Me₁—O	2	2	2.015	2.02	1.95
Me₁—O	4	2	2.092	2.08	1.99
		2	–	–	2.44
Me₂—O	2	2	2.077	2.09	1.91
Me₂—O	4	2	2.078	2.07	1.96
		2	–	–	2.61
Me₃—O	1	1	1.933	1.94	1.90
Me₃—O	1	1	2.006	2.026	1.94
Me₃—O	2	2	2.106	2.09	2.02
Me₃—O	2	1	2.126	2.11	2.39
		1	–	–	2.50
Me₄—O	2		1.969	1.96	1.90
Me₄—O	2		2.071	2.06	2.00
Me₄—O	1		2.096	2.105	2.20
Me₄—O	1		2.105	2.111	2.38
Cell parameters					
a			9.1828(3)	9.17	9.39
b			12.2766(3)	12.31	12.02
c			3.0091(1)	2.9978	3.14

compounds is not high since at a large concentration of Cu ions, there would appear monoclinic distortions in the crystals due to the Jahn-Teller effect. Assuming the Vegard's law for the lattice parameters to be true, we estimate the concentrations of Cu ions to be lower than 10 percent.

As noted above, the Cu ions are Jahn-Teller ions. All the oxygen octahedra around the Cu ions in Cu_2MnBO_5 are extended, whereas the oxygen octahedra around the Ni ions in Ni_2MnBO_5 are compressed (Table 2). In the studied samples all the oxygen octahedra around the metallic ions are similar to those in Ni_2MnBO_5, which confirms the low concentration of Cu ions in the compounds. However, the Me_2 oxygen octahedra demonstrate a weak tendency to extension. We suppose that the Cu ions in these compounds primarily occupy the position of Me_2.

4. Magnetic properties

The magnetic properties of the single crystal $(Ni,Cu)_2MnBO_5$ were measured using the PPMS-9 Physical Property Measurement System (Quantum Design) within the temperature range of 3–300 K in the magnetic fields 0.1–80 kOe. The measurements were carried out in two directions. In the first case, the magnetic field was applied along the needle, which corresponds to the c axis of the crystallographic cell. In the second case, the magnetic field was applied perpendicular to the needle, which corresponds to the *ab* plane of the crystallographic cell.

The magnetization increases below 75 K (Fig. 3). When the external field is applied perpendicular to the needle, the magnetization is similar in all the conditions, namely zero field-cooled (ZFC), field-cooled (FC), and field-cooled heating (FCH) (Fig. 3). A slight difference between the FC and ZFC curves is observed in the temperature range of 25–75 K.
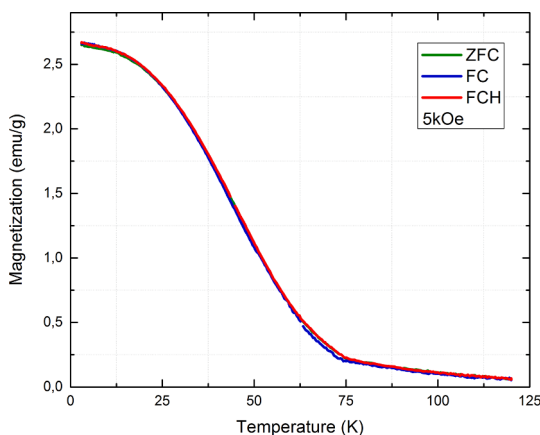

Fig. 2. The ludwigite structure.

Fig. 3. The magnetization in the zero-field-cooled (ZFC), field-cooled (FC), and field-cooled-heating (FCH) conditions measured at H = 5 kOe, which is applied perpendicular to the needle.

Fig. 5. The M-H hysteresis loops measured at different temperatures in the ZFC condition in the external field applied perpendicular to the needle.

Fig. 6. The M-H hysteresis loops measured at different temperatures in the ZFC condition in the external field applied along the needle.

When the external field is applied along the needle, the magnetization is similar only in the FC and FCH conditions (Fig. 4). In this case, the difference between the FC and ZFC curves is significant at all the temperatures below 75 K (See Fig. 4).

The field dependences of magnetization show that the ferromagnetic (or ferrimagnetic) ordering appears below 75 K in the *ab* plane (See Fig. 5). It is likely that one of the magnetic subsystems is ferrimagnetically ordered and its magnetic moments are oriented perpendicular to the needle (Fig. 3, 4, 5 and 6). The magnetic system of ludwigites is often divided into two subsystems. The first subsystem is formed by the ions in positions 2 and 4. The second subsystem is formed by the ions in positions 3 and 1. In Fe_3BO_5 [5] and in Cu_2MnBO_5 the magnetic moments of the ions inside the subsystems are oriented antiferromagnetically, while the magnetic moments of two subsystems are oriented orthogonally in Fe_3BO_5 [5], or at an angle of 60 degrees in Cu_2MnBO_5 [10]. We assume that a part of the magnetic moments in the studied compound should be antiferromagnetically oriented due to the greatest value of magnetization being small or the magnetic ordering being not complete because magnetization in the field applied along the needle in the ZFC and FC regimes is different and there is no saturation of magnetization.

On the whole, the temperature and field dependences of magnetization of $(Ni,Cu)_2MnBO_5$ are similar for Ni_2MnBO_5 with a few exceptions. In Ni_2MnBO_5 there are two features on the temperature dependence of magnetization at 85 and 71 K, while in $(Ni,Cu)_2MnBO_5$ a single feature is observed. Moreover, the coercive field in $(Ni,Cu)_2MnBO_5$ increases smoothly with the decreasing temperature.

5. Heat capacity

The heat capacity measurements were performed on an adiabatic unit, which is a simplified version of the adiabatic calorimeter described in detail in [16] without an external temperature control screen. The measurements were made within the range from 15 K to 100 K in a cryostat placed in a bath with liquid helium, and above 100 K in a cryostat placed in a bath with liquid nitrogen.

The sample consisted of a set of crystals with the total weight of 222.5 mg, sealed in an aluminum container, which, in turn, was placed in a cryostat cell. The "Apiezon N" vacuum lubricant was used to provide thermal contact. The heat capacity of this system was measured separately without the sample, to be taken into account when calculating the heat capacity of the sample.

The heating rates ranged from 0.01 to 0.5 K/min. The temperature dependence of the specific heat capacity is shown in Fig. 7. The data were processed by a linear combination of the Debye and Einstein functions from 15 to 200 K. (Eq. (1)).

$$f(T,a) := a_0 \cdot \left(\frac{T}{a_1}\right)^3 \int_0^{\frac{a_1}{T}} x^4 \cdot \frac{exp(x)}{(exp(x)-1)^2} dx + a_2 \cdot \left(\frac{a_3}{T}\right)^2 \frac{exp\left(\frac{a_3}{T}\right)}{\left(exp\left(\frac{a_3}{T}\right)-1\right)^2} \quad (1)$$

The parameters of these functions are the following: $a_1 = 292$ K (Debye temperature), $a_3 = 607$ K (Einstein temperature), $a_0 = 0.97$ J/(g*K), $a_2 = 0.44$ J/(g*K) (weight coefficients).

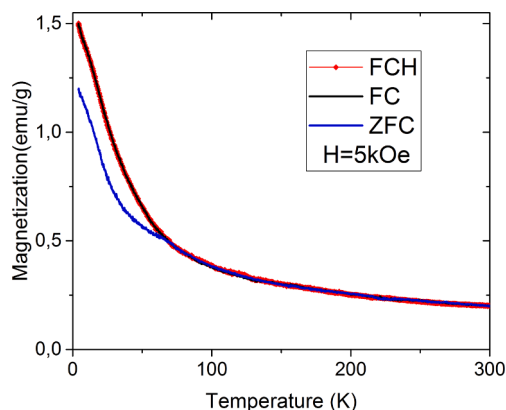To analyze the magnetic properties, a comparison was made of $\Delta Cp/$

Fig. 4. The magnetization in ZFC, FC and FCH conditions measured at H = 5 kOe, which is applied along the needle.

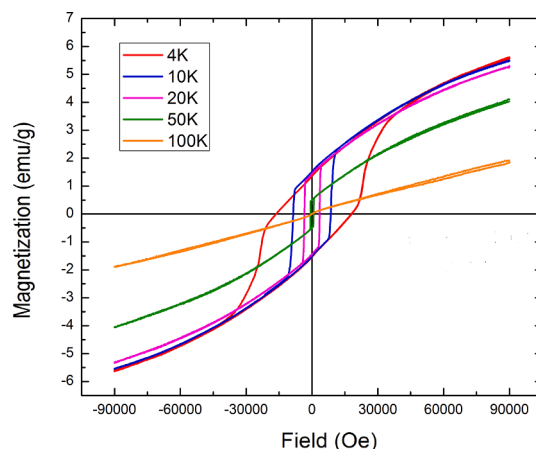**Fig. 7.** The temperature dependences of the specific heat capacity. The experimental data are denoted by the red line, and the lattice part of the heat capacity is shown by the black line.

T and dM^2/dT (Fig. 8). The $\Delta Cp/T$ was defined as the ratio of the difference between the total and excess heat capacities to the temperature. As follows from the thermodynamic relations, $\Delta Cp/T$ is proportional to dM^2/dT.

There are two features on the heat capacity curve, the first is very weak at about 75 K, and the second is at about 20 K. It is interesting that dM^2/dT agrees with $\Delta Cp/T$ when the external field is applied along the needle (the pink line in Fig. 8), but with the external field applied perpendicular to needle (the blue line in Fig. 8) dM^2/dT has its maximum at about 35 K.

In ludwigites, despite the fact that they are semiconductors or dielectrics, the specific heat in the zero field at low temperature is well fitted by two power laws, linear and square in temperature. This type of behavior was previously observed in other magnetic oxyborates [17]. In particular, the investigation of the transport properties of Co_3BO_5 shows that this compound can be classified as a Mott–Hubbard insulator [18]. But the specific heat of Co_3BO_5 is described by the power laws with linear and square terms [19]. The linear term is generally associated with disorder due to the large magnetic frustration present in these systems [20]. The square term is attributed to magnetic elementary excitations with a linear dispersion in the nearly 2D antiferromagnetic system, which was observed in another Ni-based 2D frustrated magnet [21]. The specific heat capacity of the studied compound does not show any feature which is similar to the classical λ-peak. We assume that the features on the specific heat curves associated with the magnetic

ordering are very broad. Such behavior of the heat capacity was found in ludwigite $Co_5Ti(O_2BO_3)_2$. In [20] it is assumed that the magnetic state in this compound is spin glasses due to magnetic frustration.

In the studied compound only a single feature was found on the magnetization curves, but the specific heat demonstrates small features at 75 K and a broad peak at around 20 K. The method used allows measurements of the heat capacity only at 15 K and above. Therefore, to correctly process the data, additional measurements at lower than 15 K are needed. It can be assumed that a part of the magnetic moments is ordered at 75 K, but when the temperature decreases, other magnetic moments begin to order but there is still no full long-range order in the studied compound.

6. Exchange interactions and discussion

The exchange interactions in Cu_2MnBO_5 and Ni_2MnBO_5 were analyzed in [11,13] in the framework of the Andersen-Zawadsky's indirect exchange model [22,23]. The model parameters were taken from [23]. Assuming that position 2 is occupied by Cu^{2+} (x = 0.1) and by Ni^{2+} (x = 0.9) we estimated the exchange interaction in $(Ni,Cu)_2MnBO_5$. The calculation results and the comparison with Ni_2MnBO_5 are shown in Fig. 9.

The substitution of the Ni ions in position 2 with Cu ions leads to an increase in the ferromagnetic exchange interactions 2–2 and 2–3 and to a decrease in the antiferromagnetic exchange interaction 2–4. Such changes in the exchange interactions lead to increasing frustrations in the system which could result in a decrease in the temperature of magnetic ordering. This is in agreement with the experimental data, which show that the temperature of magnetic ordering in Ni_2MnBO_5 is higher than that in $(Ni,Cu)_2MnBO_5$.

An increase in chemical disorder affects the magnetic properties in different ways, depending on the type of the magnetic ion added to the system. In $Ni_{2.14}Mn_{0.86}BO_5$, where a part of the nickel ions is substituted with tetravalent manganese, the temperature of magnetic ordering increases to 100 K but the coercive field is lower than 500 Oe. In the studied compound, where a part of the nickel ions is substituted with Cu ions, the temperature of magnetic ordering decreases, but the coercive field increases. As is mentioned above, in ludwigites metal ions form triangular groups, which generate a geometric prerequisite for

Fig. 8. The comparison of $\Delta C_p/T$ (green line) and dM^2/dT for magnetization when the external field is applied along (pink line) and perpendicular (blue line) to the needle.

Fig. 9. The comparison of the exchange interactions (in Kelvin) in (Ni, Cu)$_2$MnBO$_5$ and Ni$_2$MnBO$_5$.

frustrations appearing in the system. When a part of the ions is substituted with magnetic or nonmagnetic ions, the balance of the exchange interactions changes. The substitution of Ni with Cu leads to the enhanced ferromagnetic interactions and to a decrease in the antiferromagnetic interactions. As a result, the compound $(Ni,Cu)_2MnBO_5$ is more magnetically hard than Ni_2MnBO_5.

7. Conclusion

The single crystals of $(Ni,Cu)_2MnBO_5$ were grown by the flux technique. The crystal structure of this compound belongs to the space group Pbam(55). The analysis of the structural data shows that the content of the copper ions in the crystal is lower than 10 percent. The magnetic ordering is observed in the ferrimagnetic phase at 75 K. In contrast to $(Ni,Mn)_3BO_5$, in $(Ni,Cu)_2MnBO_5$ there is a single feature on the magnetization curves but the heat capacity shows two features which are broad. We assume that only a part of magnetic moments is ordered at 75 K, but when the temperature decreases, other magnetic moments begin to order, though there is still no full long range order in the studied compound.

Declaration of Competing Interest

The authors declare that they have no known competing financial interests or personal relationships that could have appeared to influence the work reported in this paper.

References

[1] S. Sofronova, I. Nazarenko, Ludwigites: From natural mineral to modern solid solutions, Cryst. Res. Technol. 52 (4) (2017) 1600338, https://doi.org/10.1002/crat.v52.410.1002/crat.201600338.

[2] J. Paul Attfield, J.F. Clarke, D.A. Perkins, Magnetic and crystal structures of iron borates, Physica B 180-181 (1992) 581–584.

[3] R.B. Guimarães, M. Mir, J.C. Fernandes, M.A. Continentino, H.A. Borges, G. Cernicchiaro, M.B. Fontes, D.R.S. Candela, E.M. Baggio-Saitovitch, Cationmediated interaction and weak ferromagnetism in $Fe_3O_2BO_3$, Phys. Rev. B 60 (1999) 6617.

[4] M.A. Continentino, J.C. Fernandes, R.B. Guimarães, H.A. Borges, A. Sulpice, J.-L. Tholence, J.L. Siqueira, J.B. da Cunha, C.A. dos Santos, Magnetic interactions inthe monoclinic ludwigite $Cu_2FeO_2BO_3$, Eur. Phys. J. B 9 (1999) 613–618.

[5] P. Bordet, E. Suard, Magnetic structure and charge ordering in Fe_3BO_5: a singlecrystal x-ray and neutron powder diffraction study, Phys. Rev. B 79 (2009), 144408.

[6] S.N. Sofronova, L.N. Bezmaternykh, E.V. Eremin, I.I. Nazarenko, N.V. Volkov, A.V. Kartashev, E.M. Moshkina, The superexchange interactions and magnetic ordering in low-dimentional ludwigite $Ni_5GeB_2O_{10}$, J. Magn. Magn. Mater. 401 (2016) 217–222.

[7] L.N. Bezmaternykh, E.M. Kolesnikova, E.V. Eremin, S.N. Sofronova, N.V. Volkov, M.S. Molokeev, Magnetization pole reversal of ferrimagnetic ludwigites $Mn_{3-x}Ni_xBO_5$, J. Magn. Magn. Mater. 364 (2014) 55–59.

[8] D.C. Freitas, C.P.C. Medrano, D.R. Sanchez, R.M. Nuñez, J.A. Rodríguez-Velamazán, M.A. Continentino, Magnetism and charge order in the ladder compound $Co_3O_2BO_3$, Phys. Rev. B 94 (2016), 174409.

[9] Y.V. Knyazev, N.V. Kazak, I.I. Nazarenko, S.N. Sofronova, N.D. Rostovtsev, J. Bartolome, A. Arauzo, S.G. Ovchinnikov, Effect of magnetic frustrations on magnetism of the Fe_3BO_5 and Co_3BO_5 ludwigites, J. Magn. Magn. Mater. 474 (2019) 493–500.

[10] E. Moshkina, C. Ritter, E. Eremin, S. Sofronova, A. Kartashev, A. Dubrovskiy, L. Bezmaternykh, Magnetic structure of Cu_2MnBO_5 ludwigite: thermodynamic, magnetic properties and neutron diffraction study, J. Phys.: Condens. Matter 29 (2017) 245801.

[11] S. Sofronova, E. Moshkina, I. Nazarenko, Y. Seryotkin, S.A. Nepijko, V. Ksenofontov, K. Medjanik, A. Veligzhanin, L. Bezmaternykh, Crystal growth, structure, magnetic properties and theoretical exchange interaction calculations of Cu_2MnBO_5, J. Magn. Magn. Mater. 420 (2016) 309–316.

[12] K. Bluhm, H. Muller-Buschbaum, Zur stabilisierung der Oxidationsstufe M^{IV} in $Ni_5MB_2O_{10}$-Typ Z. anorg, Allg. Chem. (1989) 111–115.

[13] E. Moshkina, S. Sofronova, A. Veligzhanin, M. Molokeev, I. Nazarenko, E. Eremin, L. Bezmaternykh, Magnetism and structure of Ni_2MnBO_5 ludwigite, J. Magn. Magn. Mater. 402 (2016) 69–75.

[14] S. Sofronova, E. Moshkina, I. Nazarenko, A. Veligzhanin, M. Molokeev, E. Eremin, L. Bezmaternykh, Chemical disorder reinforces magnetic order in ludwigite (Ni, Mn)$_3B_O5$ with Mn4+ inclusion, J. Magn. Magn. Mater. 465 (2018) 201–210.

[15] G.M. Sheldrick, Acta Crystallogr. Sect. A 46 (1990) 467–473.

[16] A.V. Kartashev, I.N. Flerov, N.V. Volkov, K.A. Sablina, Phys. Solid State 50 (2008) 2115.

[17] D.C. Freitas, R.B. Guimarães, J.C. Fernandes, M.A. Continentino, C.B. Pinheiro, J.A. L.C. Resende, G.G. Eslava, L. Ghivelder, Phys. Rev. B 81 (2010), 174403.

[18] N.B. Ivanova, A.D. Vasilyev, D.A. Velikanov, N.V. Kazak, S.G. Ovchinnikov, G. A. Petrakovskii, V. Rudenko, Phys. Solid State 49 (2007) 651.

[19] D.C. Freitas, M.A. Continentino, R.B. Guimaraes, J.C. Fernandes, J. Ellena, L. Ghivelder, Phys. Rev. B 77 (18) (2008), 184422.

[20] D.C. Freitas, R.B. Guimaraes, D.R. Sanchez, J.C. Fernandes, M.A. Continentino, J. Ellena, A. Kitada, H. Kageyama, A. Matsuo, K. Kindo, et al., Phys. Rev. B 81 (2010), 024432.

[21] S. Nakatsuji, Y. Nambu, H. Tonomura, O. Sakai, S. Jonas, C. Broholm, H. Tsunetsugu, Y. Qiu, Y. Maeno, Science 309 (2005) 1697.

[22] P.W. Anderson, New approach to the theory of superexchange interactions, Phys. Rev. 115 (1) (1959) 2–13.

[23] O.A. Bayukov, A.F. Savitskii, The prognostication possibility of some magnetic properties for dielectrics on the basis of covalency parameters of ligandcation bonds, Physica Status Solidi (b) 155 (1989) 249–255.